^{120}Sn homologous levels via the ^{123}Sb($\vec{p}$, α)^{120}Sn reaction: Experimental evidence and microscopic calculations

P. Guazzoni and L. Zetta
Dipartimento di Fisica dell' Università, and
Istituto Nazionale di Fisica Nucleare, Via Celoria 16, I-20133 Milano, Italy

B. F. Bayman
School of Physics and Astronomy, University of Minnesota, Minneapolis, Minnesota, USA

A. Covello and A. Gargano
Dipartimento di Scienze Fisiche, Università di Napoli Federico II, and Istituto Nazionale di Fisica Nucleare, Complesso Universitario di Monte S. Angelo, Via Cintia, I-80126 Napoli, Italy

G. Graw and R. Hertenberger
Sektion Physik der Ludwig-Maximilians-Universität München, D-85748 Garching, Germany

H.-F. Wirth
Physik Department, Technische Universität München, D-85748 Garching, Germany

M. Jaskola
Soltan Institute for Nuclear Studies, Warsaw, Poland
(Received 4 March 2005; published 27 October 2005)

The ^{123}Sb($\vec{p}$, α)^{120}Sn reaction has been studied in a high resolution measurement at incident energy of 24 MeV using a polarized proton source and a Q3D spectrometer. The differential cross sections and asymmetries for transitions to levels of ^{120}Sn homologous to the lowest energy states of ^{119}In have been measured and interpreted in terms of the experimental differential cross sections and asymmetries of the parent ^{119}In states, on the basis of the weak-coupling model. Several (17) states of the ^{120}Sn residual nucleus, not previously reported in the literature, have been detected and spins and parities have been proposed for seven of them, while parities have been proposed for five other previously known levels. In order to analyze the transitions populating the homologous levels, for both differential cross sections and asymmetries, microscopic DWBA calculations have been performed using spectroscopic amplitudes obtained from a shell-model study.

DOI: 10.1103/PhysRevC.72.044604 PACS number(s): 21.10.Hw, 21.60.Cs, 25.40.Hs, 27.60.+j

I. INTRODUCTION

The ($\vec{p}$, α) reaction on nuclei around singly or doubly closed shells displays several properties that make it a useful spectroscopic tool for supplementing level structure information obtained by other charged-particle reactions. In our previous work concerning $Z = 40$ [1,2] and $Z = 82$ regions [3,4], we have shown that an interesting behavior can be observed for a number of transitions induced by ($\vec{p}$, α) reactions on near-magic target nuclei having one nucleon outside a completely filled major shell. In this case the unpaired slightly-bound nucleon may act as spectator in the process.

The ($\vec{p}$, α) reaction on near-magic target nuclei (odd-A nuclei) having one nucleon outside a completely filled major shell is characterized by some distinctive features:

(i) weak population of residual nucleus levels below an excitation energy strictly related to the energy gap in the nucleon single-particle spacing at the filling of the major shell,
(ii) excitation of states with a close structural relationship (homologous states) of residual nuclei from ($\vec{p}$, α) reaction on adjacent target nuclei, one *magic* with a magic neutron and/or proton shell (leading to parent transition) and the other *near-magic* with one more nucleon (spectator) outside the major shell (leading to a multiplet of corresponding daughter states).

As shown in our previous studies [1,3], the homology concept allows for the odd-mass target nuclei to single out a dominant transition amplitude and, consequently, to identify spin, parity, and configuration.

In the case of the ($\vec{p}$, α) reaction on odd-mass target nuclei and for transitions to states with spin values different from 0, several l and j transfers may contribute to each transition, which have to be added incoherently in a DWBA calculation. In the case of homologous states, one has only one l and j transfer, that is given by the transition to the corresponding parent state.

In this work, we have studied the ^{123}Sb($\vec{p}$, α)^{120}Sn reaction leading to multiplets of states which are homologous to the lowest energy states of ^{119}In (parent states). Angular distributions of cross sections and asymmetries for transitions

to the latter were measured in a previous study [5] of the $(\vec{p}, \alpha)$ reaction on the target nucleus ^{122}Sn. To identify homologous levels in ^{120}Sn, we compare these distributions with those measured in the present experiment (see Sec. III).

In order to analyze the transitions populating the homologous levels for both differential cross sections and asymmetries, microscopic DWBA calculations have been performed using spectroscopic amplitudes obtained from a shell model study of the 22- and 20-neutron systems outside the $N = 50$ major neutron shell, in ^{123}Sb target nucleus and ^{120}Sn residual nucleus, respectively. The shell-model calculations of the motion of these neutrons have been performed within the framework of the seniority scheme using a realistic effective interaction derived from the Paris free nucleon-nucleon potential [6]. The model space has been truncated to states with seniority less than or equal to 4 [7].

As a result of our study of the ^{123}Sb$(\vec{p}, \alpha)^{120}$Sn reaction, the experimental information about the ^{120}Sn levels has been improved. From the experimental point of view the level structure of ^{120}Sn nucleus has been extensively studied by means of different kinds of nuclear reactions, expecially those induced by light projectiles. In particular, the level scheme of ^{120}Sn has been investigated by means of inelastic scattering of protons [8,9], deuterons [10], ^{3}He and α [11,12], lithium ions [13,14], and by using the following one-, two-, and multinucleon transfer reactions ^{119}Sn(d, p) [15,16], ^{119}Sn(t, d) [17], ^{121}Sb $(d,^3$He) [18], ^{121}Sb(t, α) [19], ^{122}Sn(p, t) [7,20], ^{118}Sn(t, p) [21], ^{123}Sb(p, α) measured with low energy resolution [22], and ^{124}Te$(d,^6$Li) [23]. The most comprehensive information is obtained from γ-ray spectroscopy using the (n, γ), $(n, n'\gamma)$, (γ, γ'), $(P, P'\gamma)$ reactions [24–27] and Coulomb excitation [27,28] as well as from the study of the decay of ^{120}In [29–32] and ^{120}Sb [29,33,34]. The results obtained in these works are summarized in the NDS compilation [35], where a more complete list of references can be found.

This paper is organized as follows. In Sec. II the experimental procedure and the results are described. In Sec. III the experimental evidence of the multiplets of ^{120}Sn homologous levels is discussed. Microscopic calculations of spectroscopic amplitudes and $(\vec{p}, \alpha)$ transfer amplitudes are reported in Sec. IV. Section V is devoted to the summary. In the Appendix the calculation of the three nucleon-transfer spectroscopic amplitudes is described. A brief preliminary report of the present work has been given elsewhere [36].

II. EXPERIMENTAL PROCEDURE AND RESULTS

The ^{123}Sb$(\vec{p}, \alpha)^{120}$Sn reaction has been studied at 24 MeV incident energy with the HVEC MP Tandem accelerator of the University and Technical University of Munich, using the new source for negative polarized D^- and H^- hydrogen ion beams. The Stern-Gerlach source [37] with electron-cyclotron resonance (ECR) ionizer and Cesium vapour target for charge exchange was able to produce proton beams with intensity up to 1.5 μA on the target. In our experiment the value of the polarization was 0.6.

The 50 μg/cm^2 thick ^{123}Sb isotopically enriched (98.28%) target was evaporated onto an 8 μg/cm^2 carbon backing. The reaction products were momentum separated by the Q3D magnetic spectrograph, at nine angles between 6° and 52.5°, with both spin-up and spin-down polarization in different magnetic field settings in order to reach an excitation energy of the residual nucleus of 4750 keV. The setting of the spectrograph entrance slits provided a solid angle of 2.98 msr for $\theta = 6°$ and a solid angle of 11.04 msr for $\theta \geqslant 10°$.

Outgoing α particles were identified by the new proportional counter [38] with cathode-strip readout for the Q3D focal plane, designed to detect light ions such as p, d, t, α with a position resolution of better than 0.1 mm, good particle identification and high count rate. The particles were stopped in a 7 mm thick plastic scintillator (NE-104) which ensured both ΔE-E particle identification and good position resolution.

The good energetic characteristics of the accelerator, the spectrograph, and the focal plane detector allowed for the measurement of high-resolution energy spectra. The energy resolution was 12 keV FWHM in the detection of the outgoing α particles.

In Fig. 1 the energy spectrum of α particles measured at 20° is shown. The spectrum shown at top of the figure combines the measurements of the two magnetic settings used for the ^{123}Sb$(\vec{p}, \alpha)^{120}$Sn reaction and covers the energy range from 0 to ~4800 keV. The portion of the spectrum between channels 0 and 300, corresponding to the homologous region, is presented in the middle of the figure. At the bottom of the figure, the parent states populated at low excitation energy in the ^{122}Sn$(\vec{p}, \alpha)^{119}$In reaction are shown, in order to display corresponding homologous levels in both ^{119}In and ^{120}Sn residual nuclei. The excitation of the most prominent peaks is indicated. The excitation energies were determined through the calibration of the spectra using a polynomial of rank 2, whose parameters were set by reproducing the excitation energies of 15 levels determined in γ-decay experiments [35] and identified in our α spectra. Quoted energies are estimated to have an uncertainty of 3 keV.

All spectra were normalized with respect to the beam current accumulated by a Faraday cup and analyzed with the AUTOFIT shape fitting code [39]. The shape of the α peak at 3695 keV was used as reference for both spin-up and spin-down spectra. The absolute cross section for each α peak was calculated from its area, taking into account effective target thickness, solid angle, and collected charge and was estimated with a systematic uncertainty of 15%. The favorable peak to background ratio, the high resolving power of the magnetic spectrograph, the large solid angle, and the spectrum energy resolution allowed us to measure rather weakly populated levels having cross section values as low as 1μb/sr at the maximum of the angular distribution.

A total of 61 transitions to the final states of ^{120}Sn up to 4739 keV excitation energy have been measured. Several (17) states, not previously reported in the literature [35], have been detected and spins and parities have been assigned to seven of them, while parities to five others.

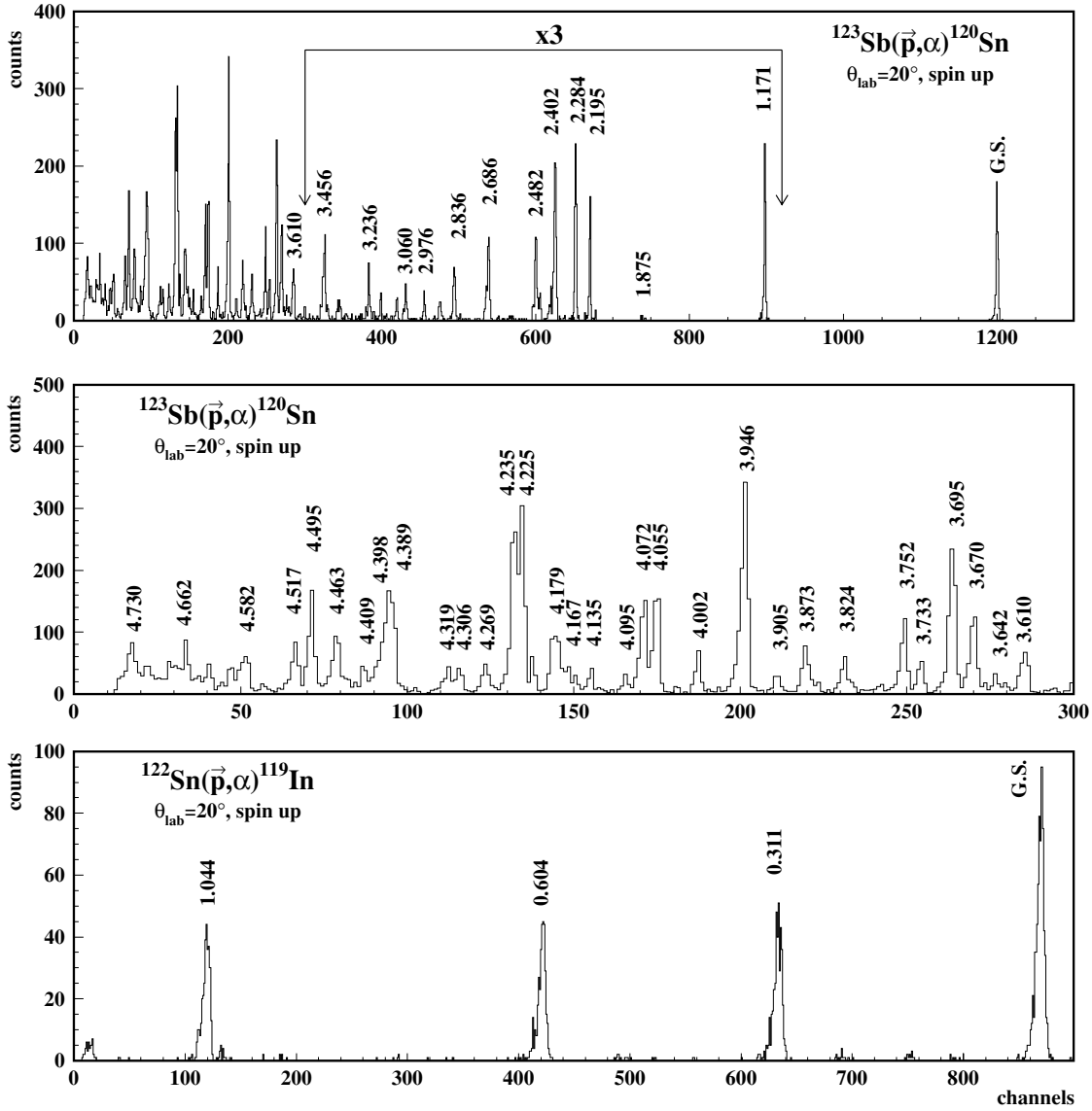

FIG. 1. Energy spectra of α particles measured at 20° for the ^{123}Sb($\vec{p}$, α)^{120}Sn and ^{122}Sn($\vec{p}$, α)^{119}In reactions. In the spectrum of the ^{123}Sb($\vec{p}$, α)^{120}Sn reaction (top) the portion between arrows indicates that the number of shown counts is multiplied by a factor of 3. The portion of the spectrum of the ^{123}Sb($\vec{p}$, α)^{120}Sn reaction between channel 0 and channel 300 (homologous region) is enlarged in the middle. At the bottom, the parent states of the ^{122}Sn($\vec{p}$, α)^{119}In reaction are presented.

The excitation energies, spins and parities of the ^{120}Sn levels identified in the present work are shown in Table I, together with the corresponding adopted values. Column 5 reports the experimental cross sections, integrated from 6° to 52.5°, and the corresponding statistical errors. This table is relevant in connection with the need to acquire a large body of data to test and confirm nuclear structure models. It also points to an interesting feature of the completeness of the spectroscopic information provided by different reactions. Neutron capture and fusion reactions are generally supposed to populate all levels, whereas the (p, α) reaction is supposed to be selective. In spite of the supposed selectivity of (p, α) reactions, we have studied states of ^{120}Sn hardly identified in other less selective reactions.

III. ^{120}Sn LEVELS HOMOLOGOUS TO THE LOWEST ENERGY STATES OF ^{119}In

In the α spectrum of the ^{123}Sb($\vec{p}$, α)^{120}Sn reaction reported in Fig. 1, it is possible to recognize two different regions: the homologous region ($E_{ex} \geqslant 3.6$ MeV) intensively populated, and the low-excitation energy region poorly populated by the pickup of the $0_{g_{7/2}}$ spectator proton and a neutron pair.

The dominant contribution arises from a process in which the incident proton picks up a proton and a pair of neutrons from the core, while the valence proton outside the $Z = 50$ shell acts as a spectator. In this higher excitation energy region, multiplets of states have been identified. The configurations of these multiplets result from the coupling of the spectator proton

TABLE I. In columns 1 and 2 are listed the adopted energies, spins, and parities [35] of the ^{120}Sn levels and in column 3 the energies observed in the present work; in column 4 the spins and/or parities of the levels observed in the present work are reported, and, in case of fragmented levels, the J^π of the corresponding missed member of the multiplet is shown in square brackets; in column 5 the integrated cross sections from 6° to 52.5°, estimated with a systematic error of ±15%, are reported together with the statistical errors; in column 6 the energies of the ^{119}In parent states are indicated. Our quoted energies are estimated to have an uncertainty of ±3 keV.

Adopted [35]		Present work			Parent
E_x (keV)	J^π	E_x (MeV)	J^π	$\sigma_{\rm int}(\mu b)$	state ^{119}In
0	0^+	0	0^+	12.4 ± 0.5	
1171.265	2^+	1.171		4.9 ± 0.3	
1875.108	0^+	1.875		—	
2097.205	2^+	2.098		—	
2159.931	0^+	2.160		—	
2173					
2194.299	4^+	2.195		3.8 ± 0.3	
2284.27	5^-	2.284		7.3 ± 0.4	
2297	$0^+,1^+$				
2355.383	2^+	2.356		—	
2400.30	3^-	2.402		8.1 ± 0.4	
2420.90	2^+				
2465.632	4^+	2.462		1.6 ± 0.2	
2481.63	7^-	2.482		4.1 ± 0.2	
2540	(5^-)				
2587.25	0^+				
2643.353	4^+				
2685.16	6^+	2.686		4.3 ± 0.2	
2691	$(2^+$ and $6^+)$				
2695.94	4^-				
2728.12	2^+				
2749.71	6^-				
2751	4^+				
2800.05	5^-				
2802	$(7^-,8^+)$				
2835.39	1^+				
2836.52	(8^+)	2.836		3.1 ± 0.2	
2844.34	$(6)^-$				
2857.61	(0^+)				
2902.22	(10^+)	2.900		2.0 ± 0.2	
2930.53	2^+				
2975.69	4^-	2.976		1.1 ± 0.1	
2997					
3009	2^+				
3034.75	(0^+)				
3057.946	4^+	3.060		1.3 ± 0.1	
3069.73	(6^+)				
3077.38	3^+				
3100	(1^-)	3.104		0.8 ± 0.1	
3157.97	2^+				
3179.06	4^+	3.179		1.5 ± 0.1	
3208.54	0^+				
3210	$1^+,2^+,3^+$				
3231.95	$1^+,2^+,3^+$				
		3.236		1.6 ± 0.1	
3237.32	(1,2)				
3252	5^-				
3262.89					
3279.29	(1^-)				
3284.62	2^+				
3330	$(6^+,7^-)$				
3341					
3349.92	$(4)^+$				
3386.32	2^+	3.380		1.2 ± 0.1	
3438.23	4^+				
3446.48	$(7^-,8^-)$	3.456		3.6 ± 0.2	
3455					
3471.54	3^-				
3547.58	1,2				
3559					
3581.90	(1,2)				
3600		3.610	2^+	7.5 ± 0.3	g.s.
3631.14	2^+				
3644.48	$(6^+,7^-)$	3.642		4.1 ± 0.2	
		3.670	4^+	13.4 ± 0.4	g.s.
		3.695	7^+	23.0 ± 0.5	g.s.
3711.01	(1,2)				
		3.733		4.1 ± 0.2	
		3.752	3^+	10.3 ± 0.4	g.s.
3765.31	$1^+,2^+$				
3772.09	+				
3777.21	4^+	3.778		2.1 ± 0.2	
		3.824		5.5 ± 0.3	
3835.36	2^+				
3857.56	(4)	3.858		3.0 ± 0.2	
3874.95	2^+	3.873		6.2 ± 0.3	
3906.6	-	3.905	2^-	2.9 ± 0.2	1.044
3928					
3955		3.946	8^+	29.3 ± 0.6	g.s.
3990.1	$(2)^+$				
4006.5	(1,2)	4.002	$-[3^-]$	3.6 ± 0.2	0.311
4011.4	(1,2)				
		4.055	4^-	12.2 ± 0.4	0.311
4079	$1^+,2^+,3^+$	4.072	$+[6^+]$	11.6 ± 0.4	g.s.
4096.5		4.095	1^-	2.3 ± 0.2	1.044
4110.4	$0^-,1^-$				
		4.135		3.3 ± 0.2	
4146.9					
		4.167	1^+	5.7 ± 0.3	g.s.
4180	–	4.179	3^-	10.5 ± 0.4	0.604
4190	$1^+,2^+,3^+$				
		4.225		28.5 ± 0.6	
4230	+				
		4.235		11.6 ± 0.4	
		4.269	$-[3^-]$	3.3 ± 0.2	0.311
		4.306	$-[3^-]$	3.5 ± 0.2	0.311
4318.2	$0^-,1^-$	4.319		2.5 ± 0.2	
4360	–	4.389	4^-	14.7 ± 0.4	0.604
		4.398	$-[6^-]$	7.7 ± 0.3	1.044
4410	–	4.409	3^-	4.4 ± 0.2	1.044

TABLE I. (*Continued.*)

Adopted [35] E_x (keV)	J^π	Present work E_x (MeV)	J^π	$\sigma_{\rm int}$ (μb)	Parent state ^{119}In
4460	–	4.463	+ [6$^+$]	10.9 ± 0.4	g.s.
		4.495	5$^+$	15.0 ± 0.4	g.s.
		4.517	4$^-$	7.8 ± 0.3	1.044
		4.558	−[6$^-$]	1.9 ± 0.2	1.044
4580		4.582	2$^-$	7.3 ± 0.3	0.604
		4.603	−[5$^-$]	4.3 ± 0.2	0.604
		4.630	−[5$^-$]	6.0 ± 0.3	0.604
4650	–	4.654	−[5$^-$]	3.2 ± 0.2	0.604
		4.662		8.8 ± 0.3	
4690	–	4.684		6.4 ± 0.3	
		4.713	−[5$^-$]	6.2 ± 0.3	0.604
4720					
		4.730	5$^-$	8.1 ± 0.3	
		4.739		4.5 ± 0.2	

(not involved in the process) with the low-lying states excited in the ^{119}In core that we call parent states.

In the case of weak coupling between the parent state and the spectator nucleon it is expected that

(i) the angular distributions of cross sections and analyzing powers for transitions to homologous states are very similar in shape because the processes exciting these states are essentially the same;
(ii) the differential cross section for populating a parent state is approximately equal in magnitude to the sum of the cross sections (cumulative cross section) of the transitions to the multiplet of homologous states corresponding to the given parent state;
(iii) the relative cross section for the population of a homologous state with spin J_i in a given multiplet is proportional to $(2J_i + 1)$.

Starting from ∼3.6 MeV of excitation energy in ^{120}Sn we have identified levels homologous to the lowest energy levels of ^{119}In by comparing angular distributions of cross sections and asymmetries with the respective distributions for the following parent states in ^{119}In, i.e., $\frac{9}{2}^+$ g.s., $\frac{1}{2}^-$ 0.311 MeV, $\frac{3}{2}^-$ 0.604 MeV, and $\frac{5}{2}^-$ 1.044 MeV [5]. The angular distributions of cross sections and asymmetries of these parent states are significantly different from each other, and this allows a reliable discrimination between the multiplets of homologous states.

We assigned the spin values to the ^{120}Sn homologous levels following the $(2J + 1)$ rule. Because of the coupling of the $0g_{7/2}$ proton with the positive or negative parity parent states, the parity of the ^{120}Sn daughter states is positive or negative, respectively.

In Table I knowledge about multiplets of identified homologous states is summarized:

(i) seven levels (1$^+$, 2$^+$, 3$^+$, 4$^+$, 5$^+$, 7$^+$, 8$^+$) homologous to the $\frac{9}{2}^+$ g.s. of ^{119}In (an octet is expected, whose spins range from 1$^+$ to 8$^+$);
(ii) one level (4$^-$) homologous to the $\frac{1}{2}^-$ 0.311 MeV state of ^{119}In (a doublet is expected, whose spin values are 3$^-$ and 4$^-$);
(iii) three levels (2$^-$, 3$^-$, 4$^-$) homologous to the $\frac{3}{2}^-$ 0.604 MeV state of ^{119}In (a quartet is expected, whose spin values range from 2$^-$ to 5$^-$);
(iv) five levels (1$^-$, 2$^-$, 3$^-$, 4$^-$, 5$^-$) homologous to the $\frac{5}{2}^-$ 1.044 MeV state of ^{119}In (a sextet is expected, whose spin values range from 1$^-$ to 6$^-$).

In Table I, the levels with only parity assignment are assumed to result from fragmentation of missing members of the multiplet, as discussed below.

In Figs. 2, 3, 4 and 5 we compare the experimental $\sigma(\theta)$ and $A_y(\theta)$ angular distributions for the transitions to the multiplets in ^{120}Sn with those for the transition to the corresponding parent level in ^{119}In, $\sigma(\theta)$ being scaled for each level i by the spin factor $\frac{2J_i+1}{(2J_c+1)(2j+1)}$, where J_c is the spin of the parent state, and j is the spin of the 51$^{\rm st}$ $(0g_{7/2})$ proton in the ^{123}Sb target nucleus.

Spin and parity 1$^+$, 2$^+$, 3$^+$, 4$^+$, 5$^+$, 7$^+$, 8$^+$ are attributed to the 4.167 MeV, 3.610 MeV, 3.752 MeV, 3.670 MeV, 4.495 MeV, 3.695 MeV, 3.946 MeV, respectively, homologous to the $\frac{9}{2}^+$ g.s. of ^{119}In. The 2$^+$ 3.610 MeV level may coincide with the 3.600 MeV level reported on the adopted level scheme [35], without attribution of spin and parity and observed in ^{118}Sn(t, p)^{120}Sn at (3593±15)keV [21], and in the ^{119}Sn(d, p)^{120}Sn reaction at 3600 keV [15]. The observed 3.946 MeV 8$^+$ level presumably coincides with the (3955±10) keV listed in Ref. [35] without spin and parity attribution, which is observed in (p, p') reaction [8]. The remaining levels of the septet are not reported in Ref. [35].

The level at 4.055 MeV is identified as the 4$^-$ member of the doublet of states of ^{120}Sn homologous to the $\frac{1}{2}^-$ 0.311 MeV state of ^{119}In. This level was not seen previously. We do not observe the 3$^-$ member of this doublet.

We have identified three states of ^{120}Sn homologous to the $\frac{3}{2}^-$ 0.604 MeV state of ^{119}In at 4.179, 4.389, and 4.582 MeV, respectively. The first level could correspond to the reported level [35] at 4180 keV, observed in (t, α) and $(d,{}^3{\rm He})$ reactions. The other two levels could correspond to 4360 keV, and 4580 keV levels observed in the $(d,{}^3{\rm He})$ reaction [35]. Negative parity is reported for the 4180 keV and 4360 keV levels, while the level at 4580 keV is quoted without spin and parity assignment.

We assign 1$^-$, 2$^-$, 3$^-$, 4$^-$, and 5$^-$, respectively, to the five states identified as homologous to the $\frac{5}{2}^-$ 1.044 MeV state of ^{119}In, at 4.095, 3.905, 4.409, 4.517, and 4.730 MeV. The level at 4.517 MeV is not reported in Ref. [35]. The remaining levels may correspond to the levels reported in the compilation of Kitao [35] at 4096.5 keV and 3906.6 keV observed in $(n, n'\gamma)$ and in $(d,{}^3{\rm He})$ and (t, α) reactions, and 4410 keV and 4720 keV populated in the $(d,{}^3{\rm He})$ and (t, α) reactions. Negative parity is reported for the 3906.6 keV and 4410 keV levels.

If the differential cross sections for the transitions belonging to the same multiplet are summed, the cumulative experimental

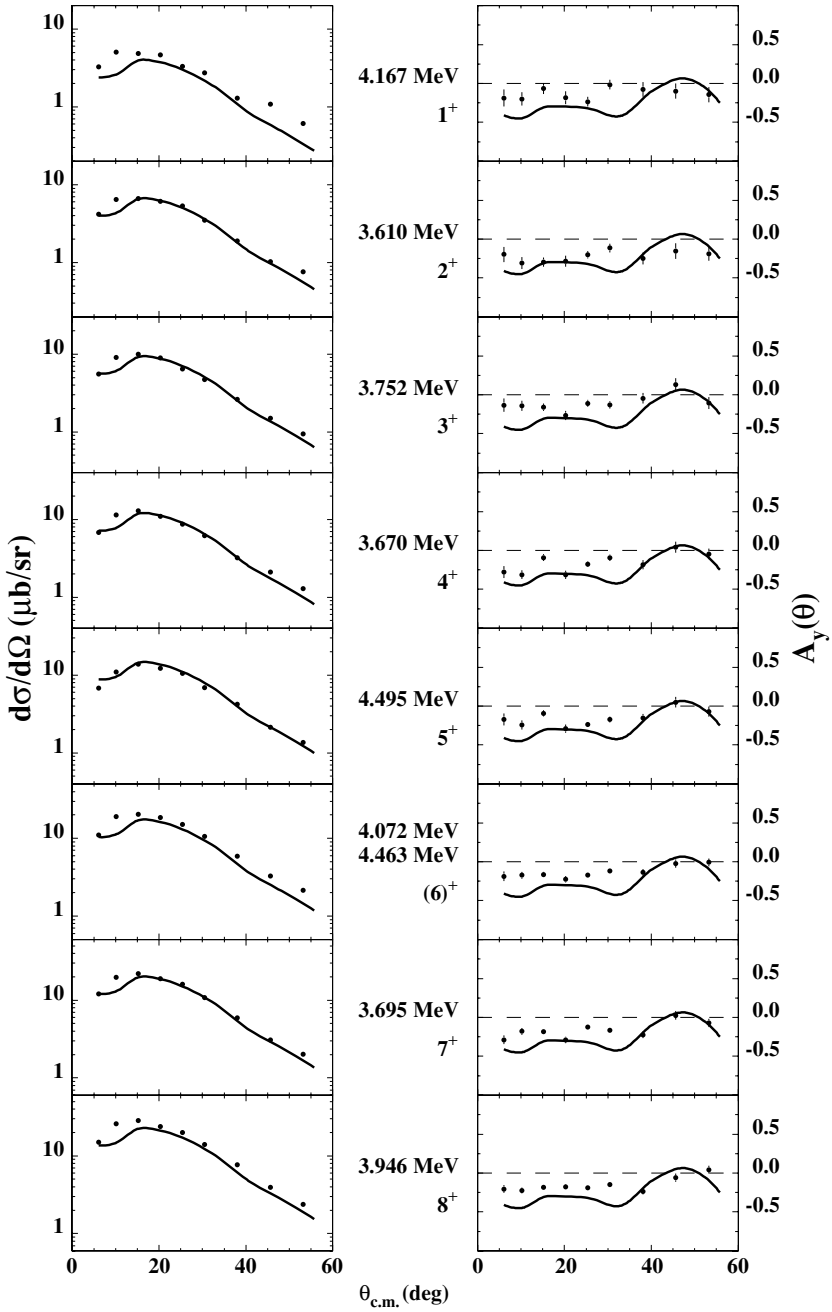

FIG. 2. Experimental cross sections and analyzing powers for the population of the ^{120}Sn levels, homologous to the $\frac{9}{2}^+$ ground state of ^{119}In, compared with the experimental cross section [scaled according to the $(2J_i + 1)$ rule with the J_i value shown] and analyzing power, for the population of the ground state (solid line).

cross section is obtained. On the basis of the weak coupling model, this cumulative cross section must be equal in magnitude to the differential cross section for population of its parent state. In the present case the cumulative cross sections for all the multiplets of states homologous to the ^{119}In parent states do not exhaust the corresponding parent cross sections, due to the fact that some members of each multiplet are missing.

In the expected octet of states homologous to the $\frac{9}{2}^+$ ^{119}In ground state, the 6^+ state is missing. The cross section of the 6^+ member is expected to be about 16% of the cumulative cross section of the multiplet, but in our work there is no experimental evidence for a peak with such a cross section. On the contrary, the shapes of the differential cross sections and asymmetries of the 4.072 MeV and 4.463 MeV levels of ^{120}Sn fit the corresponding shapes of the parent state very well. The ^{120}Sn adopted level scheme [35] reports a level at 4079 keV with $J^\pi = 1^+, 2^+, 3^+$, observed in the $(n, n'\gamma)$ reaction [26], which may correspond to our 4.072 MeV level, and a level at 4460 keV with negative parity deduced from $L = 1$ transfer in $(d, ^3\mathrm{He})$ reaction, that probably does not correspond to our 4.463 MeV level (to which we attribute positive parity). The 4.072 MeV and 4.463 MeV levels are the fragments of the 6^+ homologous state and if the differential cross sections for the excitation of these two levels are added to the $\sigma(\theta)$ of the septet of states unambigously identified as homologous to the $\frac{9}{2}^+$ ^{119}In ground state the cumulative cross section practically coincides with that of the parent $\frac{9}{2}^+$ ^{119}In ground state.

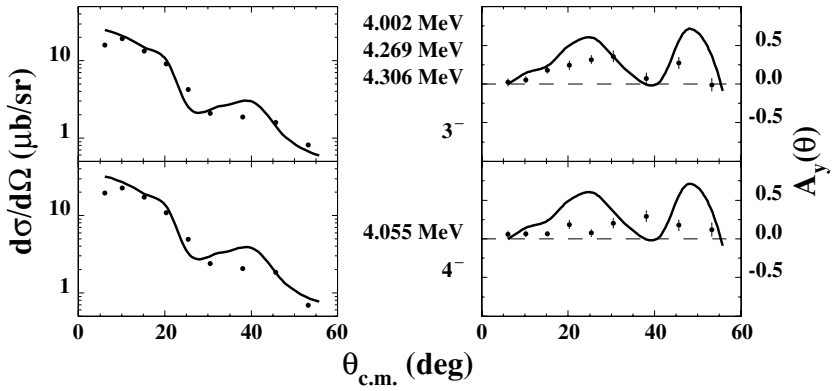

FIG. 3. Same as Fig. 2 but for population of the levels of ^{120}Sn homologous to the $\frac{1}{2}^-$ 0.311 MeV level of ^{119}In.

In the case of the expected doublet of states homologous to the 0.311 MeV $\frac{1}{2}^-$ level of ^{119}In, the 3^- member is missing, with an expected cross section of ∼44% of the multiplet cumulative cross section. However the shapes of $\sigma(\theta)$ and $A_y(\theta)$ of the 4.002, 4.269, and 4.306 MeV levels of ^{120}Sn are reproduced very well by the corresponding shapes of the parent state. At 4.000 MeV a level is identified from $(d,{}^3\mathrm{He})$ [18] and (t,α) [19] transfer reactions with $(2)^+$ assignment and reported in the adopted level scheme [35] at an energy of 3990.1 keV. A level at 4006.5 keV without parity assignment is also reported in the adopted level scheme [35]. Probably our level at 4.002 MeV, to which we assign negative parity, does not correspond to the 3990.1 keV level, but may correspond to the level at 4006.5 keV. The ±20 keV uncertainty on the adopted 4280 keV energy value allows us to conclude that the level we identify at 4.269 MeV may coincide with the adopted one listed in Ref. [35] without spin and parity assignment, while the level at 4.306 MeV has no correspondence in the adopted level scheme [35]. The sum of the differential cross sections for all the transitions belonging to the expected doublet exhausts the $\sigma(\theta)$ of the 0.311 MeV $\frac{1}{2}^-$ parent state of ^{119}In.

In the expected quartet of states homologous to the $\frac{3}{2}^-$ 0.604 MeV state of ^{119}In, the 5^- member is missing. Its expected cross section represents about 34% of the multiplet cumulative cross section. The 4.603, 4.630, 4.654, and 4.713 MeV levels seems to be the fragments of the 5^-, as deduced from the comparison of the shape of their $\sigma(\theta)$ and $A_y(\theta)$ with the parent ones. Moreover if the $\sigma(\theta)$ for the population of these four states are added to the $\sigma(\theta)$ of the three states unambiguously identified as homologous, the cumulative cross section of the multiplet reproduces the differential cross section of the parent $\frac{3}{2}^-$ 0.604 MeV state of ^{119}In state. In the adopted level scheme of ^{120}Sn, the 4650±10 keV and the 4690±20 keV levels, observed in the $(d,{}^3\mathrm{He})$ and (t,α) reactions with $L = 1$ transfer, are reported with negative parity and may correspond to our levels at 4.654 and 4.713 MeV, respectively, while the 4.603, 4.630 MeV levels we observe are not reported.

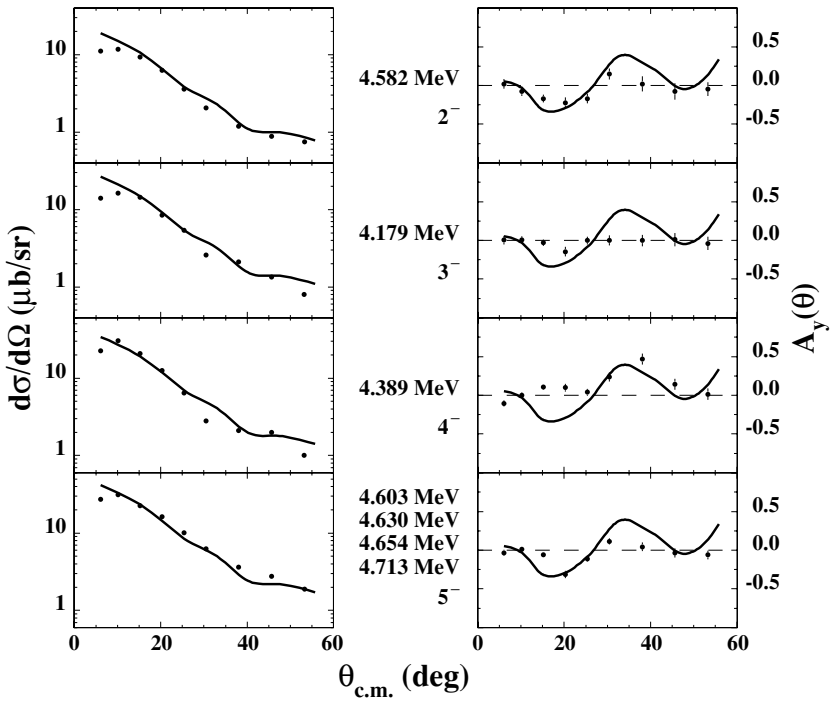

FIG. 4. Same as Fig. 2 but for population of the levels of ^{120}Sn homologous to the $\frac{3}{2}^-$ 0.604 MeV level of ^{119}In.

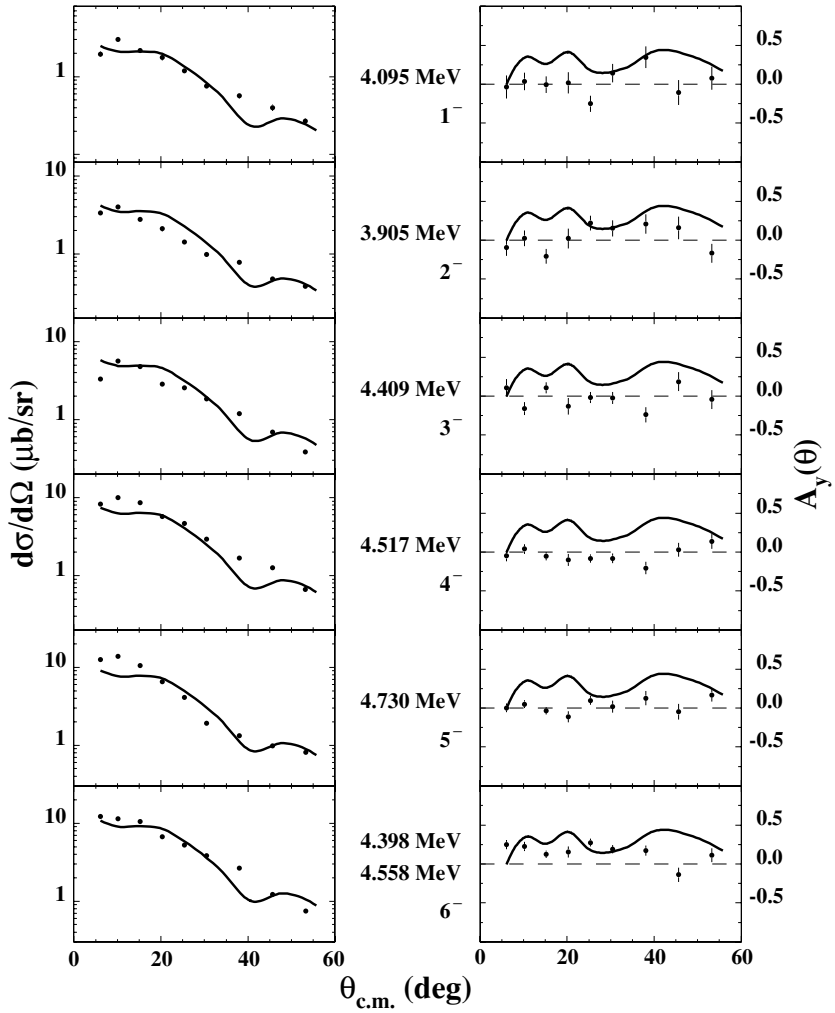

FIG. 5. Same as Fig. 2 but for population of the levels of ^{120}Sn homologous to the $\frac{5}{2}^-$ 1.044 MeV level of ^{119}In.

In the multiplet of states homologous to the $\frac{5}{2}^-$ 1.044 MeV state of ^{119}In the cross section of the 6^- missing member is about 27% of the cumulative one and we have identified the levels at 4.398, 4.558 MeV, not reported in the adopted level scheme, as fragments of this state.

In Fig. 6, we show cumulative cross sections and analyzing powers for population of multiplets of states of ^{120}Sn homologous to the low-lying parent states of ^{119}In, including the fragmented level contributions. In the same figure, for comparison, experimental cross sections and analyzing powers for population of the ^{119}In ground state, 0.311 MeV, 0.604 MeV, 1.044 MeV parent states are superimposed, showing that the cumulative cross section for each multiplet is equal in magnitude to the differential cross section for population of its parent state. This is in accord with the predictions of the weak coupling model.

As was previously stated, in the case of weak coupling between parent state and the 51st unpaired proton, the relative cross section for the population of a homologous state with spin J_i in a given multiplet must be proportional to $2J_i + 1$. In fact, the cross section of a homologous state can be related to that of the corresponding parent state by means of the expression $\sigma(J_i)_{120\mathrm{Sn}} = \frac{(2J_i+1)\sigma_{119\mathrm{In}}}{\sum_i(2J_i+1)}$. In Fig. 7 we report, as functions of J_i, the quantities $\frac{\sigma(J_i)_{120\mathrm{Sn}}}{\sigma_{119\mathrm{In}}}\sum_i(2J_i+1)$ for each multiplet of ^{120}Sn states homologous to the ^{119}In parent states we have identified, including also the fragmented members. The straight line, $(2J_i + 1)$, is also displayed. The satisfactory agreement between the experimental data (solid dots) and the prediction of the weak coupling model (dashed line) supports the spin and/or parity assignment of ^{120}Sn homologous levels.

IV. MICROSCOPIC CALCULATIONS

A. Spectroscopic Amplitudes

Calculations [40] concerning the wave function of the ground state of ^{123}Sb have shown that it is dominated (79%) by a single $g_{7/2}$ proton, coupled to a neutron state of angular momentum zero. However, there are components in which a proton in state $j_s(= g_{7/2}, d_{5/2}, d_{3/2}, s_{1/2})$ is coupled to a neutron state of angular momentum $L_n = 2$. We follow this picture and assume that the ground state is a linear combination of components in which a proton in single-particle state j_s is coupled to a neutron state of angular momentum L_n (= 0, 2) to yield the ^{123}Sb ground state angular momentum of 7/2. The

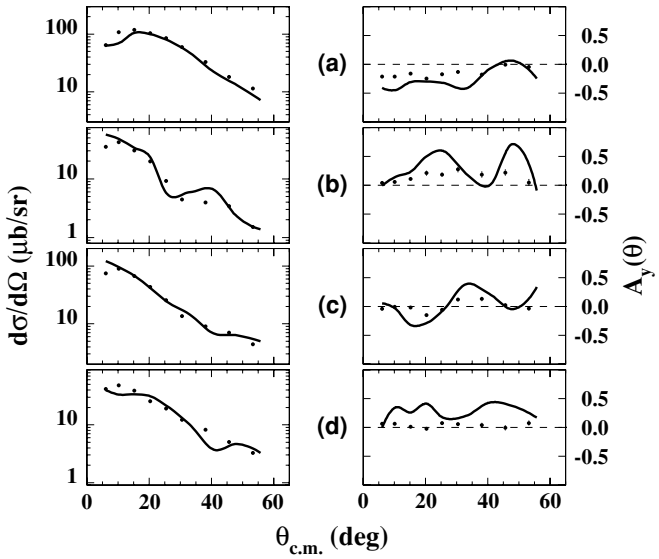

FIG. 6. Cumulative cross sections and analyzing powers for population of multiplets of states of ^{120}Sn (solid dots), homologous to the low-lying parent states of ^{119}In, including the fragmentated level contributions, are compared with the cross sections and analyzing powers for population of these ^{119}In states (solid lines): (a) for the multiplet homologous to the ^{119}In ground state, (b) for the multiplet homologous to the ^{119}In 0.311 MeV level, (c) for the multiplet homologous to the ^{119}In 0.604 MeV level, (d) for the multiplet homologous to the ^{119}In 1.044 MeV level.

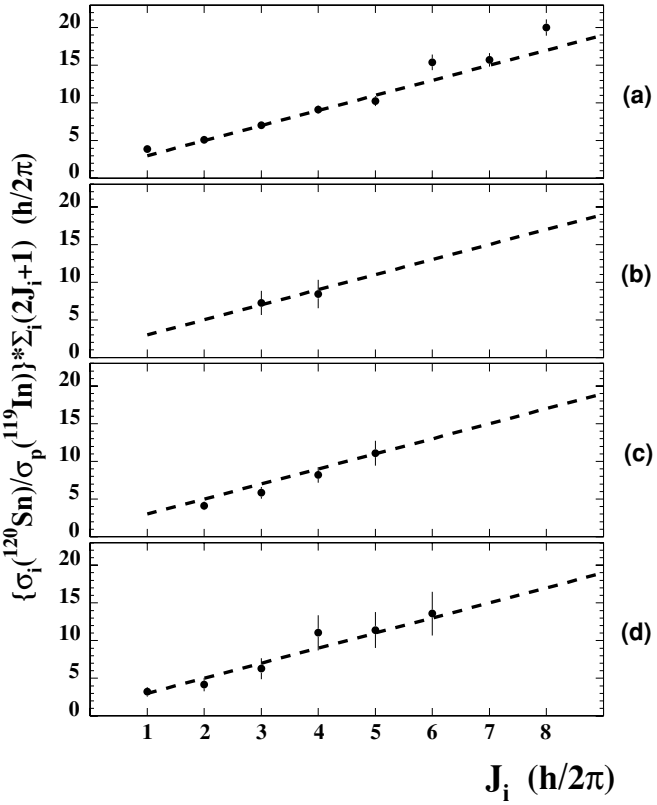

FIG. 7. Experimental values $\frac{\sigma(J_i)^{120}\mathrm{Sn}}{\sigma^{119}\mathrm{In}}\sigma_i(2J_i+1)$ (dots) for each member of the multiplets of states homologous to the ^{119}In parent states are reported as a function of J_i and compared with the straight line $(2J_i + 1)$ predicted by the weak coupling model (dashed lines): (a) for the multiplet homologous to the ^{119}In ground state, (b) for the multiplet homologous to the ^{119}In 0.311 MeV level, (c) for the multiplet homologous to the ^{119}In 0.604 MeV level, (d) for the multiplet homologous to the ^{119}In 1.044 MeV level.

amplitudes of these components are taken from the work of Hooper *et al*. [40].

The 22 neutrons outside the $N = 50$ major neutron shell closure are assumed to move in the $0g_{7/2}$, $1d_{5/2}$, $1d_{3/2}$, $2s_{1/2}$, and $0h_{11/2}$ shells. We have performed a shell-model study of the motion of these neutrons within the framework of the so-called chain-calculation method, which is a nonconventional approach to shell-model problems within the seniority scheme. A description of this approach can be found in Ref. [7]. In the present calculations we have included states with seniority up to 4. It may be mentioned that we have compared the results obtained by this approach with those of complete shell-model calculations for Sn isotopes with up to ten valence particles or holes. It has turned out that our approximation scheme yields energies of the low-lying yrast states which are only a few percent away from the exact ones. As residual interaction between the valence neutrons outside doubly magic ^{100}Sn, we have used a two-particle effective interaction derived from the Paris nucleon-nucleon potential. An account of how this derivation is performed is given in Ref. [41].

The neutron single-particle energies have been taken directly from the experimental spectrum of ^{131}Sn. The five levels observed in this nucleus below 2.5 MeV excitation energy are, according to the conclusions of Refs. [42,43], single-neutron hole states. Their corresponding energies are (in MeV) $\epsilon^{-1}_{d_{3/2}} = 0.0$, $\epsilon^{-1}_{h_{11/2}} = 0.242$, $\epsilon^{-1}_{s_{1/2}} = 0.332$, $\epsilon^{-1}_{d_{5/2}} = 1.655$, and $\epsilon^{-1}_{g_{5/2}} = 2.434$. The single-particle energies can be obtained [44] from these values through

$$\epsilon_j = -(\epsilon^{-1} + \Delta_j),$$

with

$$\Delta_j = \frac{1}{2j+1}\sum_{j'J}(2J+1)G_J(jj'jj'),$$

where the G's are the matrix elements of the two-body effective interaction between states that are antisymmetrized but not normalized. In this way we obtain the following values (in MeV): $\epsilon_{g_{7/2}} = 0.0$, $\epsilon_{d_{5/2}} = 0.591$, $\epsilon_{d_{3/2}} = 2.382$, $\epsilon_{s_{1/2}} = 2.141$, and $\epsilon_{h_{11/2}} = 2.988$.

If the (p, α) reaction removes the $0g_{7/2}$ proton, the resulting ^{120}Sn nucleus is, in this picture, a $Z = 50$ proton closed-shell core plus 20 neutrons outside the $N = 50$ major neutron shell. We have also done a shell-model study of this 20-neutron system [7]. These states of ^{120}Sn represent the *nonhomologous* states. However, if the (p, α) reaction removes a proton from the filled $0g_{9/2}$, $0f_{5/2}$, $1p_{3/2}$, or $1p_{1/2}$ shells, the residual ^{120}Sn nucleus has a $0g_{7/2}(nlj)^{-1}$ proton configuration. The states populated in this way can be regarded as a $0g_{7/2}$ proton coupled to an $(n, l, j)^{-1}$ proton hole state in ^{119}In. We refer to these

states as *homologous* states. In the case of $0g_{9/2}$ proton pickup, for example, the result is a $0g_{7/2}(0g_{9/2})^{-1}$ proton configuration, which gives rise to even-parity levels with angular momenta $J_f = 1, 2, 3, 4, 5, 6, 7$, and 8. Similarly, if a $1p_{3/2}$ proton is removed, the result is the proton configuration $0g_{7/2}(1p_{3/2})^{-1}$, which gives rise to odd-parity levels with angular momenta $J_f = 2, 3, 4$, and 5. As regards the neutron configuration of each multiplet, this is expected to be the same as that of the parent state in ^{119}In.

The definition and notation of the spectroscopic amplitude is given in the Appendix, where there is also a derivation of the relation between two-nucleon and three-nucleon spectroscopic amplitudes. The principal result for the spectroscopic amplitude for the population of the homologous state of angular momentum J_f composed of a proton in particle state j_s coupled to a proton hole in state j_h is

$$S\left([j_s L_n]^{7/2} \xrightarrow{\{[j_1 j_2]^{L_n} j_h\}^J} [j_s j_h^{-1}]^{J_f}\right) = -(-1)^{L_n + j_s - 7/2}\sqrt{\frac{2J_f+1}{2j_s+1}}\,U(L_n j_h 7/2 J_f; J 7/2) \times \langle\tilde{0}|\Psi_m^{L_n}\frac{[n^{\dagger j_1} n^{\dagger j_2}]_m^{L_n}}{\sqrt{1+\delta_{j_1 j_2}}}\Psi_0^{\dagger 0}|\tilde{0}\rangle C_{j_s,L_n}. \quad (1)$$

Here the neutrons have been transferred from the single-particle states j_1, j_2, and the total angular momentum transferred is J. The final factor C_{j_s,L_n} is the amplitude of the component of the ^{123}Sb ground state consisting of a j_s proton coupled to an L_n neutron state, and

$$\langle\tilde{0}|\Psi_m^{L_n}\frac{[n^{\dagger j_1} n^{\dagger j_2}]_m^{L_n}}{\sqrt{1+\delta_{j_1 j_2}}}\Psi_0^{\dagger 0}|\tilde{0}\rangle$$

is the two-neutron spectroscopic amplitude corresponding to the L_n neutron state of ^{123}Sb and the assumed $L_n = 0$ neutron state of ^{120}Sn. The two-neutron spectroscopic amplitudes corresponding to the $L_n = 0$ and $L_n = 2$ components of ^{123}Sb are calculated from our shell-model wave functions for ^{122}Sn and ^{120}Sn. It will be seen that the $L_n = 2$ amplitudes make a much smaller contribution to the cross section than do the $L_n = 0$ amplitudes. All the spectroscopic amplitudes used in this calculation are given in Table II.

The differential cross section and asymmetry are incoherent sums over the allowed values of angular momentum transfer J. However, the terms of different L_n, j_s, j_1, j_2 contribute coherently. The situation is especially simple when the $L_n = 0$ terms dominate this coherent sum. Then Eq. (1) reduces to

$$S\left([j_s 0]^{7/2} \xrightarrow{\{[j_1 j_2]^0 j_h\}^J} [j_s j_h^{-1}]^{J_f}\right) = -\delta_{j_s,7/2}\delta_{j_1,j_2}\delta_{J,j_h} \times \sqrt{\frac{2J_f+1}{8}}\langle\tilde{0}|\Psi_0^0\frac{[n^{\dagger j_1} n^{\dagger j_1}]_0^0}{\sqrt{2}}\Psi_0^{\dagger 0}|\tilde{0}\rangle C_{7/2,0}. \quad (2)$$

Here only a single angular momentum transfer $J = j_h$ contributes, and this J is the same for all values of J_f, from $J_f = |j_h - j_s|$ to $j_h + j_s$. This implies that (p, α) reactions populating all the states homologous to the j_h hole state in ^{119}In will have angular distributions with the same shapes. Furthermore, in this situation, the only J_f-dependence occurs in the $\sqrt{2J_f+1}$ factor, which implies that the cross sections for populating these homologous states should be proportional to $2J_f + 1$. If L_n is not zero in Eq. (1), these features do not occur. Inspection of Fig. 2 through 7 shows that homologous states do have very nearly the same angular distribution, with cross sections proportional to $2J_f + 1$. Thus the experimental data are consistent with a picture in which $L_n = 0$ transfer is dominant. In fact, $L_n = 0$ dominance is found in all of our calculations ($\geqslant 99\%$). It occurs because the $L_n = 0$ component represents most of the ^{123}Sb ground state, and because a neutron pair coupled to angular momentum zero has the greatest overlap with the relative motion of the neutrons in the transferred pair. This $L_n = 0$ dominance is also observed in two-nucleon transfer reactions [21].

TABLE II. The two-nucleon spectroscopic amplitudes, defined in Eq. (A6) of the Appendix. The relative signs of the $L_n = 0$ amplitudes are determined by the short-range nature of the neutron-neutron interaction, and our use of Condon-Shortley phases.

$n_1 l_1 j_1$	$n_2 l_2 j_2$	$L_n = 0$	$L_n = 2$
$0_{g_{7/2}}$	$0_{g_{7/2}}$	0.615	−0.0231
$0_{g_{7/2}}$	$1d_{5/2}$		−0.0172
$0_{g_{7/2}}$	$1d_{3/2}$		0.0411
$1d_{5/2}$	$1d_{5/2}$	0.567	0.0282
$1d_{5/2}$	$1d_{3/2}$		0.0138
$1d_{5/2}$	$2s_{1/2}$		0.0286
$1d_{3/2}$	$1d_{3/2}$	0.726	0.1954
$1d_{3/2}$	$2s_{1/2}$		−0.1911
$2s_{5/2}$	$2s_{1/2}$	0.528	
$0h_{11/2}$	$0h_{11/2}$	−1.318	−0.3610

As an example of transitions to nonhomologous states, we consider the ground state transition. In this case, one of the j_s protons is removed in the (p, α) reaction. Since $Z = 50$ represents a major shell closure, the proton configuration of the ground state should be well represented by a state of angular momentum zero, and therefore the 20 neutrons outside the $N = 50$ core will also have angular momentum zero. It is shown in the Appendix that the spectroscopic amplitude for reaching the ground state of ^{120}Sn is

$$S\left([j_s L_n]^{7/2} \xrightarrow{\{[j_1 j_2]^{L_n} j_s\}^J} \text{g.s.}\right) = \sqrt{\frac{8}{2j_s+1}}\langle\tilde{0}|\Psi_m^{L_n}\frac{[n^{\dagger j_1} n^{\dagger j_2}]_m^{L_n}}{\sqrt{1+\delta_{j_1 j_2}}}\Psi_0^{\dagger 0}|\tilde{0}\rangle C_{j_s,L_n}. \quad (3)$$

B. Form Factors

The calculation of the (p,α) transfer amplitude requires evaluation of the overlap between the relative motion of the transferred nucleons in their shell model orbitals, and their relative motion in the outgoing α particle. Since the assumed interaction is between the incident proton and the mass center of the three transferred nucleons, it cannot change the relative motion of the three transferred nucleons. Thus,

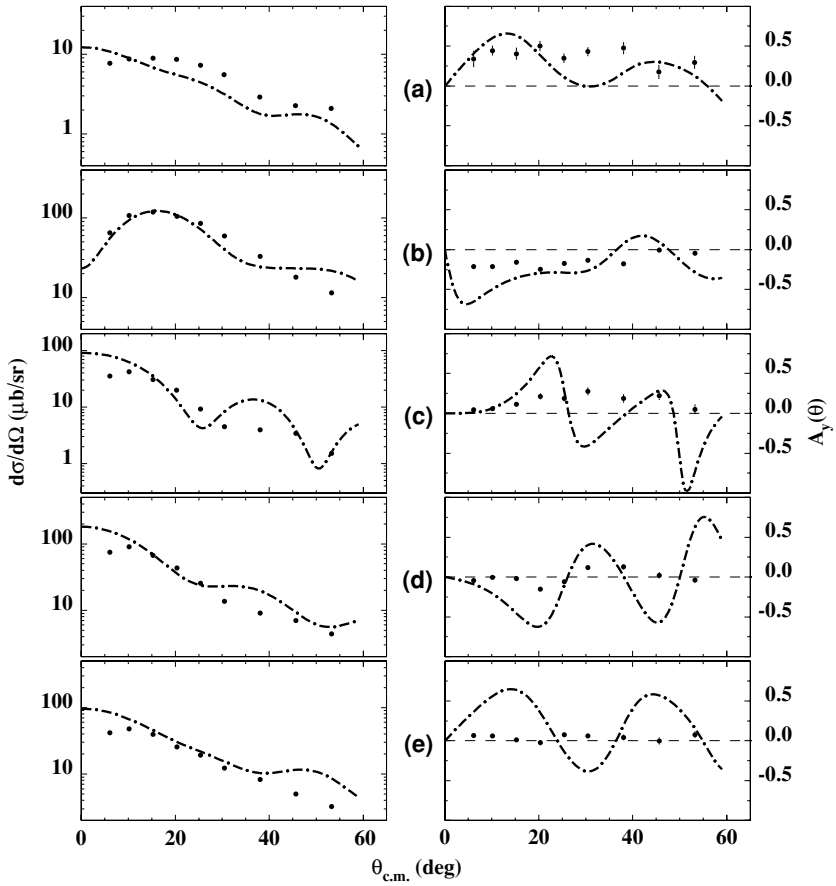

FIG. 8. The experimental angular distributions of $\sigma(\theta)$ and $A_y(\theta)$ for the transitions to the ground state of ^{120}Sn (dots) are compared in (a) with the microscopic calculation (dot-dashed lines). The ground state is a nonhomologous state obtained by removing the spectator proton. Experimental cumulative cross sections and analyzing powers for population of all multiplets of states of ^{120}Sn (dots) homologous to the low-lying parent states of ^{119}In, including the fragmented level contributions, are compared with the results of microscopic calculations (dot-dashed lines): (b) for the multiplet homologous to the ^{119}In g.s. $0g_{7/2}(0g_{9/2})^{-1}$, (c) for the multiplet homologous to the ^{119}In 0.311 MeV level $0g_{7/2}(1p_{1/2})^{-1}$, (d) for the multiplet homologous to the ^{119}In 0.604 MeV level $0g_{7/2}(1p_{3/2})^{-1}$, (e) for the multiplet homologous to the ^{119}In 1.044 MeV level $0g_{7/2}(0f_{5/2})^{-1}$.

we must project from shell-model states the part in which the three nucleons have the same relative motion as they will have in the outgoing α particle. This is done for each of the possible triples of shell-model states that can connect the initial and final states, and then a coherent sum must be taken to obtain the total transfer form factor. The theory has been described in Ref. [45]. Figure 8 illustrates the families of levels based on the $0g_{7/2}(0g_{9/2})^{-1}$, $0g_{7/2}(1p_{1/2})^{-1}$, $0g_{7/2}(1p_{3/2})^{-1}$, and $0g_{7/2}(0f_{5/2})^{-1}$ proton configurations. For each multiplet the cumulative cross section has been calculated for a hypothetical level whose excitation energy corresponds to the centroid energy of the multiplet.

In the same figure, for sake of completeness, we report also the angular distributions of $\sigma(\theta)$ and $A_y(\theta)$ for the transition to the ground state of ^{120}Sn, nonhomologous state, obtained by removing the spectator proton.

The calculations were done using the finite range distorted-wave Born approximation (DWBA), with form factors calculated from the previously described microscopic configurations. The reaction calculation was done with the code TWOFNR [46]. The optical model parameters for the proton entrance channel were deduced from a systematic survey of elastic scattering by Perey [47]; for the α-exit channel we started from the survey by McFadden and Satchler [48], and then made slight adjustments to optimize agreement with the experimental angular distributions. Table III lists the actual parameters that were used. An overall multiplicative factor was chosen to give a reasonable fit to the experimental data. It is the same for the cumulative and ground state cross sections.

It is clear from Fig. 8 that the DWBA calculations, based upon the microscopic form factors, give a good account of the relative magnitudes of the cross sections for the different multiplets. This supports our association of these multiplets with the different proton and proton-hole states in ^{120}Sn. These calculations also do a fair job of accounting for the general shapes of the angular distributions of the cross sections. However, the predicted angular distributions of the asymmetries show oscillations whose amplitudes are much larger than those exhibited by the data. Evidently, the calculated asymmetries are more sensitive to different aspects of the form factors and/or optical parameters than are the calculated differential cross sections. This is a subject that needs further investigation.

V. SUMMARY

In this paper, we have discussed the existence of homologous states in ^{119}In and ^{120}Sn observed in $(\vec{p},\alpha)$ reactions. Using the concept of homology we have been able to make seven new attributions of spin and parity and five new parity attributions, thereby improving the present knowledge of the ^{120}Sn level scheme. For negative (positive) parity low-lying states in ^{119}In, corresponding negative (positive) parity states in ^{120}Sn at relatively high excitation energy have been identified, which display a relationship of homologous states through a strict correspondence of differential cross

TABLE III. Optical model parameters used in DWBA calculations.

	V_r (MeV)	r_r (fm)	a_r (fm)	W_v (MeV)	r_v (fm)	a_v (fm)	W_d (MeV)	r_d (fm)	a_d (fm)	V_{so} (MeV)	r_{so} (fm)	a_{so} (fm)	r_c (fm)
p	52.0	1.25	0.65				8.	1.3	0.6	6.00	1.25	0.70	1.25
α	179.8	1.42	0.57	39.9	1.42	0.57							1.30

sections and asymmetries for the reactions ^{122}Sn$(\vec{p},\alpha)^{119}$In and ^{123}Sb$(\vec{p},\alpha)^{120}$Sn.

In all the identified multiplets of daughter states a member is missing; possible fragments of the missing members have been suggested and only parity assignement is made for these levels resulting from the fragmentation of missing members.

Microscopic DWBA calculations have been carried out of the cross section and asymmetry angular distributions of the transition to the ^{120}Sn 0^+ ground state, and the cumulative $\sigma(\theta)$ and $A_y(\theta)$ angular distributions of the multiplets of daughter states homologous to the ^{119}In parent states (0.0 MeV, 0.311 MeV, 0.604 MeV, 1.044 MeV). To obtain the transfer form factors we have used spectroscopic amplitudes obtained from a shell model study of the 22-neutron and 20-neutron systems outside the $N = 50$ major neutron shell, in the ^{123}Sb target nucleus and the ^{120}Sn residual nucleus, respectively. The relative cross sections and the angular distributions obtained from these microscopic DWBA calculations are in accord with the interpretation of the data in terms of homologous states.

ACKNOWLEDGMENTS

The work at the University of Naples Federico II was supported in part by the Italian Ministero dell'Istruzione, dell'Università e della Ricerca (MIUR).

APPENDIX: THE CALCULATION OF THE THREE-NUCLEON-TRANSFER SPECTROSCOPIC AMPLITUDES

Because we are concerned with hole states as well as particle states, it will be convenient to use an occupation number (second-quantized) formalism. Let $|\tilde{0}\rangle$ represent the $Z = N = 50$ doubly-closed shells. Let $(p^{\dagger j}_m, n^{\dagger j}_m)$ create, respectively, a proton or neutron in the single particle state ψ^j_m. For annihilation operators, we will use

$$\pi^j_m \equiv (-1)^{j-m} p^j_{-m}, \qquad \nu^j_m \equiv (-1)^{j-m} n^j_{-m}, \tag{A1}$$

which have rotational transformation properties indicated by j, m. The proton and neutron creation operators anticommute, as do the annihilation operators. The anticommutation relations between creation and annihilation operators imply

$$[p^{\dagger j_1}\pi^{j_2}]^I_M = -1(-1)^{j_1+j_2-I}[\pi^{j_2}p^{\dagger j_1}]^I_M - \delta_{j_1,j_2}\delta_{M,0}\delta_{I,0}\sqrt{2j_1+1}, \tag{A2}$$

$$[n^{\dagger j_1}\nu^{j_2}]^I_M = -1(-1)^{j_1+j_2-I}[\nu^{j_2}n^{\dagger j_1}]^I_M - \delta_{j_1,j_2}\delta_{M,0}\delta_{I,0}\sqrt{2j_1+1}. \tag{A3}$$

The brackets indicate vector coupling.

We consider a component of the ^{123}Sb ground state in which the proton has angular momentum $j_s (= 1g_{7/2}, 2d_{5/2}, 2d_{3/2}, 3s_{1/2})$, and the neutrons have angular momentum $L_n (= 0, 2)$. We write this state as $[p^{\dagger j_s}\Psi^{\dagger L_n}]^{7/2}_m|\tilde{0}\rangle$, where $\Psi^{\dagger L_n}_M$ represents a coupled product of 22 neutron creation operators with total angular momentum L_n. The Hermitian conjugate of this state is

$$\begin{aligned}
&\left([p^{\dagger j_s}\Psi^{\dagger L_n}]^{7/2}_m|\tilde{0}\rangle\right)^\dagger \\
&= \sum_{m_1,m_2}(j_s L_n m_1 m_2|7/2\ m)\langle\tilde{0}|\left(p^{\dagger j_s}_{m_1}\Psi^{\dagger L_n}_{m_2}\right)^\dagger \\
&= \sum_{m_1,m_2}(L_n j_s - m_2 - m_1|7/2 - m)\langle\tilde{0}|\Psi^{L_n}_{m_2}p^{j_s}_{m_1} \\
&= \sum_{m_1,m_2}(-1)^{L_n+m_2+j_s+m_1}(L_n j_s - m_2 - m_1|7/2 - m)) \\
&\quad\times\langle\tilde{0}|\Psi^{L_n}_{-m_2}\pi^{j_s}_{-m_1} \\
&= (-1)^{L_n+j_s+m}\langle\tilde{0}|[\tilde{\Psi}^{L_n}\pi^{j_s}]^{7/2}_{-m}
\end{aligned}$$

where we have defined $\tilde{\Psi}^{L_n}_m \equiv (-1)^{L_n-m}\Psi^{L_n}_{-m}$ in analogy with Eq. (A1).

We consider a final state in ^{120}Sn of angular momentum J_f consisting of the "spectator" proton with angular momentum j_s coupled to a proton hole with angular momentum j_h, with the 20 neutrons outside the $N = 50$ core coupled to angular momentum zero:

$$|^{120}\text{Sn}; J_f, M\rangle = [p^{\dagger j_s}\pi^{j_h}]^{J_f}_M\Psi^{\dagger 0}_0|\tilde{0}\rangle.$$

In this equation, $\Psi^{\dagger 0}_0$ represents a zero-coupled product of 20 neutron creation operators. The spectroscopic amplitude for a pickup reaction is defined as the scalar product of the target state with the vector coupled product of the creation operators representing the transferred nucleons and the residual state. Thus

$$\begin{aligned}
&S\left([j_s L_n]^{7/2}\ \overset{\{[j_1 j_2]^{L_n} j_h\}^J}{\longrightarrow}\ [j_s j_h^{-1}]^{J_f}\right) \\
&= (-1)^{L_n+j_s+m}\langle\tilde{0}|[\tilde{\Psi}^{L_n}\pi^{j_s}]^{7/2}_{-m} \\
&\quad\times\left[\left\{\frac{[n^{\dagger j_1}n^{\dagger j_2}]^{L_n}}{\sqrt{1+\delta_{j_1,j_2}}}p^{\dagger j_h}\right\}^J[p^{\dagger j_s}\pi^{j_h}]^{J_f}\Psi^{\dagger 0}_0\right]^{7/2}_m|\tilde{0}\rangle.
\end{aligned} \tag{A4}$$

To evaluate (A4), we note that only the angular momentum zero combination of the operator product survives between $\langle\tilde{0}|$ and $|\tilde{0}\rangle$,

$$\begin{aligned}
&\langle\tilde{0}|[\tilde{\Psi}^{L_n}\pi^{j_s}]^{7/2}_{-m}\left[\left\{\frac{[n^{\dagger j_1}n^{\dagger j_2}]^{L_n}}{\sqrt{1+\delta_{j_1,j_2}}}\pi^{\dagger j_h}\right\}^J[p^{\dagger j_s}\pi^{j_h}]^{J_f}\Psi_0^{\dagger 0}\right]^{7/2}_m|\tilde{0}\rangle\\
&\quad=(7/2\;7/2-mm|00)\\
&\qquad\times\langle\tilde{0}|\left([\tilde{\Psi}^{L_n}\pi^{j_s}]^{7/2}\left[\left\{\frac{[n^{\dagger j_1}n^{\dagger j_2}]^{L_n}}{\sqrt{1+\delta_{j_1,j_2}}}\pi^{\dagger j_h}\right\}^J\right.\right.\\
&\qquad\left.\left.\times[p^{\dagger j_s}\pi^{j_h}]^{J_f}\Psi_0^{\dagger 0}\right]^{7/2}\right)^0_0|\tilde{0}\rangle\\
&\quad=\frac{(-1)^{7/2+m}}{\sqrt{8}}\langle\tilde{0}|\left([\tilde{\Psi}^{L_n}\pi^{j_s}]^{7/2}\left[\left\{\frac{[n^{\dagger j_1}n^{\dagger j_2}]^{L_n}}{\sqrt{1+\delta_{j_1,j_2}}}\pi^{\dagger j_h}\right\}^J\right.\right.\\
&\qquad\left.\left.\times[p^{\dagger j_s}\pi^{j_h}]^{J_f}\Psi_0^{\dagger 0}\right]^{7/2}\right)^0_0|\tilde{0}\rangle. \qquad\text{(A5)}
\end{aligned}$$

Since $\psi_m^{j_h}$ is one of the occupied states in $|\tilde{0}\rangle$, we have $p^{\dagger j_h}|\tilde{0}\rangle=0$. Thus we can use Eq. (A2) to write

$$\begin{aligned}
[p^{\dagger j_h}\pi^{j_h}]^I_M|\tilde{0}\rangle&=\big(-(-1)^{j_h+j_h-I}[\pi^{j_h}p^{\dagger j_h}]^I_M\\
&\quad-\delta_{I,0}\delta_{M,0}\sqrt{2j_h+1}\big)|\tilde{0}\rangle\\
&=-\delta_{I,0}\delta_{M,0}\sqrt{2j_h+1}|\tilde{0}\rangle.
\end{aligned}$$

Then we can simplify Eq. (A5) by recoupling the angular momenta L_n, j_h, j_s, j_h to get

$$\begin{aligned}
&S\left([j_sL_n]^{7/2}\xrightarrow{\{[j_1j_2]^{L_n}j_h\}^J}[j_sj_h^{-1}]^{J_f}\right)\\
&\quad=-\sqrt{\frac{2j_h+1}{8}}\left((L_nj_h)_J(j_sj_h)_{J_f}|(L_nj_s)_{7/2}(j_hj_h)_0\right)_{7/2}\\
&\qquad\times(-1)^{L_n+j_s-7/2}\langle\tilde{0}|\left[(\tilde{\Psi}^{L_n}\pi^{j_s})^{7/2}\right.\\
&\qquad\left.\times\left\{\frac{[n^{\dagger j_1}n^{\dagger j_2}]^{L_n}}{\sqrt{1+\delta_{j_1,j_2}}}p^{\dagger j_s}\right\}^{7/2}\right]^0_0\Psi_0^{\dagger 0}|\tilde{0}\rangle\\
&\quad=-(-1)^{L_n+j_s-7/2}\sqrt{\frac{2j_h+1}{8}}\sqrt{\frac{2J_f+1}{(2j_s+1)(2j_h+1)}}\\
&\qquad\times U(L_nj_h7/2J_f;Jj_s)\\
&\qquad\times\left((L_nj_s)_{7/2}(L_nj_s)_{7/2}|(L_nL_n)_0(j_sj_s)_0\right)_0\langle\tilde{0}|\\
&\qquad\times\left[\tilde{\Psi}^{L_n}\frac{[n^{\dagger j_1}n^{\dagger j_2}]^{L_n}}{\sqrt{1+\delta_{j_1,j_2}}}\right]^0_0\Psi_0^{\dagger 0}|\tilde{0}\rangle|\langle\tilde{0}|[\pi^{j_s}p^{\dagger j_s}]^0_0|\tilde{0}\rangle.
\end{aligned}$$

Here $\left((L_nj_h)_J(j_sj_h)_{J_f}|(L_nj_s)_{7/2}(j_hj_h)_0\right)_{7/2}$ and $U(L_nj_h7/2J_f;Jj_s)$ are normalized 9-j and 6-j recoupling amplitudes.

The two-neutron spectroscopic amplitude is defined by

$$\begin{aligned}
&\langle\tilde{0}|\Psi^{L_n}_M\frac{[n^{\dagger j_1}n^{\dagger j_2}]^{L_n}_M}{\sqrt{1+\delta_{j_1,j_2}}}\Psi_0^{\dagger 0}|\tilde{0}\rangle\\
&\quad=(-1)^{L_n+M}\langle\tilde{0}|\tilde{\Psi}^{L_n}_{-M}\frac{[n^{\dagger j_1}n^{\dagger j_2}]^{L_n}_M}{\sqrt{1+\delta_{j_1,j_2}}}\Psi_0^{\dagger 0}|\tilde{0}\rangle \qquad\text{(A6)}\\
&\quad=\frac{1}{\sqrt{2L_n+1}}\langle\tilde{0}|\left(\tilde{\Psi}^{L_n}\frac{[n^{\dagger j_1}n^{\dagger j_2}]^{L_n}}{\sqrt{1+\delta_{j_1,j_2}}}\right)^0_0\Psi_0^{\dagger 0}|\tilde{0}\rangle
\end{aligned}$$

and

$$\begin{aligned}
\langle\tilde{0}|[\pi^{j_s}p^{\dagger j_s}]^0_0|\tilde{0}\rangle&=\langle\tilde{0}|-(-1)^{j_s+j_s-0}[p^{\dagger j_s}\pi^{j_s}]^0_0\\
&\quad+\sqrt{2j_s+1}|\tilde{0}\rangle=\sqrt{2j_s+1},
\end{aligned}$$

where $\pi^{j_s}_m|\tilde{0}\rangle=0$ because the state $\psi^{j_s}_m$ is not occupied in $|\tilde{0}\rangle$. Finally, we get

$$\begin{aligned}
&S\left([j_sL_n]^{7/2}\xrightarrow{\{[j_1j_2]^{L_n}j_h\}^J}[j_sj_h^{-1}]^{J_f}\right)\\
&\quad=-(-1)^{L_n+j_s-7/2}\sqrt{\frac{2j_f+1}{2j_s+1}}U(L_nj_h7/2J_f;J7/2)\\
&\qquad\times\langle\tilde{0}|\Psi^{L_n}_m\frac{[n^{\dagger j_1}n^{\dagger j_2}]^{L_n}_m}{\sqrt{1+\delta_{j_1,j_2}}}\Psi_0^{\dagger 0}|\tilde{0}\rangle. \qquad\text{(A7)}
\end{aligned}$$

Before this is used in the coherent sum over j_1, j_2, j_s, L_n, it must be multiplied by C_{j_s,L_n}, the amplitude for the occurrence of $[p^{\dagger j_s}\Psi^{\dagger L_n}]^{7/2}_m|\tilde{0}\rangle$ in the ^{123}Sb ground state.

The ^{120}Sn ground state is represented simply by $\Psi_0^{\dagger 0}|\tilde{0}\rangle$. Thus the spectroscopic amplitude for the transition from $[p^{\dagger j_s}\Psi^{\dagger L_n}]^{7/2}_m|\tilde{0}\rangle$ to the ground state is

$$\begin{aligned}
&S\left([j_sL_n]^{7/2}\xrightarrow{\{[j_1j_2]^{L_n}j_s\}^J}\text{g.s.}\right)\\
&\quad=(-1)^{L_n+j_s+m}\langle\tilde{0}|\left[\tilde{\Psi}^{L_n}\pi^{j_s}\right]^{7/2}_{-m}\\
&\qquad\times\left\{\frac{\left[n^{\dagger j_1}n^{\dagger j_2}\right]^{L_n}}{\sqrt{1+\delta_{j_1,j_2}}}p^{\dagger j_s}\right\}^{7/2}_m\Psi_0^{\dagger 0}|\tilde{0}\rangle\\
&\quad=(-1)^{L_n+j_s+m}(7/27/2-mm|00)\langle\tilde{0}|\\
&\qquad\times\left(\left[\tilde{\Psi}^{L_n}\pi^{j_s}\right]^{7/2}\left\{\frac{\left[n^{\dagger j_1}n^{\dagger j_2}\right]^{L_n}}{\sqrt{1+\delta_{j_1,j_2}}}p^{\dagger j_s}\right\}^{7/2}\right)^0_0\Psi_0^{\dagger 0}|\tilde{0}\rangle\\
&\quad=\frac{(-1)^{L_n+j_s+m-7/2-m}}{8}\left((L_nj_s)_{7/2}(L_nj_s)_{7/2}(L_nL_n)_0(j_sj_s)_0\right)_0\\
&\qquad\times\langle\tilde{0}|\left\{\tilde{\Psi}^{L_n}\frac{\left[n^{\dagger j_1}n^{\dagger j_2}\right]^{L_n}}{\sqrt{1+\delta_{j_1,j_2}}}\right\}^0_0\Psi_0^{\dagger 0}|\tilde{0}\rangle\\
&\qquad\times\langle\tilde{0}|\left\{\pi^{j_s}p^{\dagger j_s}\right\}^0_0|\tilde{0}\rangle\\
&\quad=\sqrt{\frac{8}{2j_s+1}}\langle\tilde{0}|\Psi^{L_n}_m\frac{\left[n^{\dagger j_1}n^{\dagger j_2}\right]^{L_n}_m}{\sqrt{1+\delta_{j_1,j_2}}}\Psi_0^{\dagger 0}|\tilde{0}\rangle.
\end{aligned}$$

This amplitude must also be multiplied by C_{j_s,L_n} before it is used in the coherent sum.

[1] P. Guazzoni, M. Jaskola, L. Zetta, J. Gu, A. Vitturi, G. Graw, R. Hertenberger, D. Hofer, P. Schiemenz, B. Valnion, U. Atzrott, G. Staudt, and G. Cata-Danil, Z. Phys. A **356**, 381 (1997).
[2] P. Guazzoni, M. Jaskola, L. Zetta, J. N. Gu, A. Vitturi, G. Graw, R. Hertenberger, P. Schiemenz, B. Valnion, U. Atzrott, and G. Staudt, Eur. Phys. A **1**, 365 (1998).
[3] P. Guazzoni, M. Jaskola, L. Zetta, G. Graw, R. Hertenberger, D. Hofer, P. Schiemenz, U. Atzrott, R. Neu, and G. Staudt, Phys. Rev. C **49**, 2784 (1994).
[4] J. N. Gu, A. Vitturi, C. H. Zhang, P. Guazzoni, L. Zetta, G. Graw, M. Jaskola, and G. Staudt, Phys. Rev. C **55**, 2395 (1997).
[5] P. Guazzoni, M. Jaskola, V. Yu. Ponomarev, L. Zetta, Y. Eisermann, G. Graw, R. Hertenberger, A. Vitturi, J. N. Gu, and G. Staudt, AIP Conf. Proc. No. 570 (American Institute of Physics, New York, 2001), p. 664.
[6] M. Lacombe, B. Loiseau, J. M. Richard, R. Vinh Mau, J. Coté, P. Pirès, and R. de Tourreil, Phys. Rev. C **21**, 861 (1980).
[7] P. Guazzoni, M. Jaskóla, L. Zetta, A. Covello, A. Gargano, Y. Eisermann, G. Graw. R. Hertenberger, A. Metz, F. Nuoffer, and G. Staudt, Phys. Rev. C **60**, 054603 (1999).
[8] O. Beer, A. El Behay, P. Lopato, Y. Terrien, G. Vallois, and K. K. Seth, Nucl. Phys. **A147**, 326 (1970).
[9] D. L. Allan, B. H. Armitage, and B. A. Doran, Nucl. Phys. **66**, 481 (1965).
[10] R. K. Jolly, Phys. Rev. **139**, B318 (1965).
[11] T. Yamagata, S. Kishimoto, K. Yuasa, K. Iwamoto, B. Saeki, M. Tanaka, T. Fukuda, I. Miura, M. Inoue, and H. Ogata, Phys. Rev. C **23**, 937 (1981).
[12] G. Bruge, J. C. Faivre, H. Faraggi, and A. Brussiere, Nucl. Phys. **A146**, 597 (1970).
[13] V. I. Chuev, Yu. A. Glukhov, V. I. Manko, B. G. Novatskii, A. A. Ogloblin, S. B. Sakuta, and D. N. Stepanov, Phys. Lett. **B42**, 63 (1972).
[14] A. Weller, P. Egelhof, R. Caplar, O. Karban, D. Krämer, K.-H. Möbius, Z. Moroz, K. Rusek, E. Steffens, G. Tungate, K. Blatt, I. Koenig, and D. Fick, Phys. Rev. Lett. **55**, 480 (1985).
[15] L. R. Norris and C. F. Moore, Phys. Rev. **136**, B40 (1964).
[16] E. J. Schneid, A. Prakash, and B. L. Cohen, Phys. Rev. **156**, 1316 (1967).
[17] R. Chapman, M. Hyland, J. L. Durell, J. N. Mo, M. Macphail, H. Sharma, and N. H. Merrill, Nucl. Phys. **A316**, 40 (1979).
[18] R. F. Leonard, Report No. N72-18705, 1972; NASA TM X-68004.
[19] Z. Basrak, N. Cindro, and M. Turk, Nucl. Phys. **A299**, 381 (1978).
[20] D. G. Fleming, M. Blann, H. W. Fulbright, and J. A. Robbins, Nucl. Phys. **A157**, 1 (1970).
[21] J. H. Bjerregaard, O. Hansen, O. Nathan, L. Vistisen, R. Chapman, and S. Hinds, Nucl. Phys. **Al10**, 1 (1968).
[22] E. Gadioli, E. Gadioli Erba, R. Gaggini, P. Guazzoni, P. Michelato, A. Moroni, and L. Zetta, Z. Phys. A **310**, 43 (1983).
[23] J. Jänecke, F. D. Becchetti, and C. E. Thorn, Nucl. Phys. **A325**, 337 (1979).
[24] S. Kikuchi and Y. Sugiyama, Nucl. Phys. **A223**, 1 (1974).
[25] Y. Schleringer, H. Szichman, G. Ben-David, and M. Mass, Phys. Rev. C **2**, 2001 (1970).
[26] A. M. Demidov and I. V. Mikhailov, Yad. Fiz. **55**, 865 (1992).
[27] N. G. Jonsson, A. Bäcklin, J. Kantele, R. Julin, M. Luontama, and A. Passoja, Nucl. Phys. **A371**, 333 (1981).
[28] P. H. Stelson, F. K. McGowan, R. L. Robinson, and W. T. Milner, Phys. Rev. C **2**, 2015 (1970).
[29] E. Liukkonen and J. Hattula, Z. Phys. **241**, 150 (1971).
[30] O. Scheidemann and E. Hagebo, J. Inorg. Nucl. Chem. **35**, 3055 (1973).
[31] H. C. Cheung, H. Huang, B. N. Subba Rao, L. Lessard, and J. K. P. Lee, J. Phys. G **4**, 1501 (1978).
[32] S. Raman, T. A. Walkiewicz, L. G. Multhauf, K. G. Tirsell, G. Bonsignori, and K. Allaart, Phys. Rev. C **37**, 1203 (1988).
[33] R. J. Pan, D. W. Hetherington, D. B. McConnell, and H. W. Taylor, Can. J. Phys. **48**, 1687 (1970).
[34] M. Campbell, K. W. D. Ledingham, A. D. Baillie, M. L. Fitzpatrick, J. Y. Gourlay, and J. G. Lynch, Nucl. Phys. **A249**, 349 (1975).
[35] K. Kitao, Y. Tendow, and A. Hashizume, Nucl. Data Sheets **96**, 241 (2002).
[36] P. Guazzoni, L. Zetta, A. Covello, A. Gargano, Y. Eisermann, G. Graw, R. Hertenberger, H.-F. Wirth, M. Jaskola, B. Bayman, and W. E. Ormand, AIP Conf. Proc. No. 675 (American Institute of Physics, New York, 2003), p. 686.
[37] R. Hertenberger, A. Metz, Y. Eisermann, K. El Abiary, A. Ludewig, C. Pertl, S. Trieb, H.-F. Wirth, P. Schiemenz, and G. Graw, Nucl. Instrum. Methods Phys. Res. A **536**, 266 (2005).
[38] H.-F. Wirth, H. Angerer, T. von Egidy, Y. Eisermann, G. Graw, and R. Hertenberger, Jahresbericth 2000, Beschleunigerlaboratorium München, p. 71 (2001).
[39] J. R. Comfort, ANL Physics Division, Report No. PHY 19708, Argonne.
[40] H. R. Hooper, P. W. Green, H. E. Siefken, G. C. Neilson, W. J. McDonald, D.M. Sheppard, and W. K. Dawson, Phys. Rev. C **20**, 2041 (1979).
[41] A. Covello, F. Andreozzi, L. Coraggio, A. Gargano, T. T. S. Kuo, and A. Porrino, Prog. Part. Nucl. Phys. **38**, 165 (1997).
[42] B. Fogelberg and J. Blomqvist, Phys. Lett. **B137**, 20 (1984).
[43] B. Fogelberg and J. Blomqvist, Nucl. Phys. **A429**, 205 (1984).
[44] R. D. Lawson, *Theory of Nuclear Shell Model* (Clarendon Press, Oxford, 1980), Chap. 3.
[45] B. F. Bayman, A. Evinay, C. Ellegaard, J. D. Garrett, and O. Hansen, Nucl. Phys. **A318**, 317 (1979).
[46] M. Igarashi, computer code TWOFNR (1977), unpublished.
[47] F. G. Perey, Phys. Rev. **131**, 745 (1963).
[48] L. McFadden and G. R. Satchler, Nucl. Phys. **84**, 177 (1966).